COMITATO NAZIONALE PER L'ENERGIA NUCLEARE
Laboratori Nazionali di Frascati

LNF - 67/49
17 Luglio 1967

G. Barbiellini, F. Grianti, T. Letardi and R. Visentin:

ANGULAR DISTRIBUTION OF ELECTRON PAIR PRODUCED BY POLARIZED PHOTON AT THE FRASCATI ELECTRON-SYNCHROTRON. -

(Nota interna: n. 373)

Servizio Documentazione
dei Laboratori Nazionali di Frascati del CNEN
Casella Postale 70 - Frascati (Roma)

Laboratori Nazionali di Frascati del CNEN
Servizio Documentazione

LNF-67/49

Nota Interna: n° 373
17 Luglio 1967

G. Barbiellini, F. Grianti(x), T. Letardi and R. Visentin: ANGULAR DISTRIBUTION OF ELECTRON PAIR PRODUCED BY POLARIZED PHOTON AT THE FRASCATI ELECTROSYNCHROTRON. -

Precise measurement of photon polarization in the energy range of 100 to 1000 MeV offers some difficulty because of the lack of a simple physical process to be used as good polarimeter for γ rays of such an energy. As shown by Maximon and Olsen[1], electron-positron pair production can give information on photon polarization state. The major difficulty, using electron pair production as polarimeter, arises because of the small angular aperture of the pair, at this relatively high energy, as well as the multiple scattering of the produced pair in the converter that averages the natural angular distribution.

In order to acquire detailed knowledge on the possibility of the electron pair production to be used as a proper polarimeter we have done a measurement of 150 MeV photon polarization by measuring the angular distribution of the electron pair by using two wide gap-spark chambers placed beside the Frascati pair spectrometer.

(x) - Sezione di Genova dell'INFN, Genova.

THE EXPERIMENTAL APPARATUS. -

The polarized γ-ray beam, whose polarization we analize, is the coherent bremsstrahlung beam from the 1 - GeV electrons striking a diamond target. This beam is now a facility of the Frascati elec tronsynchrotron.

The γ-beam is transferred from a synchrotron straight sec tion to the aluminium converter placed within the pair spectrometer as sketched in Fig. 1. The goniometer which holds the diamond target is within the straight section.

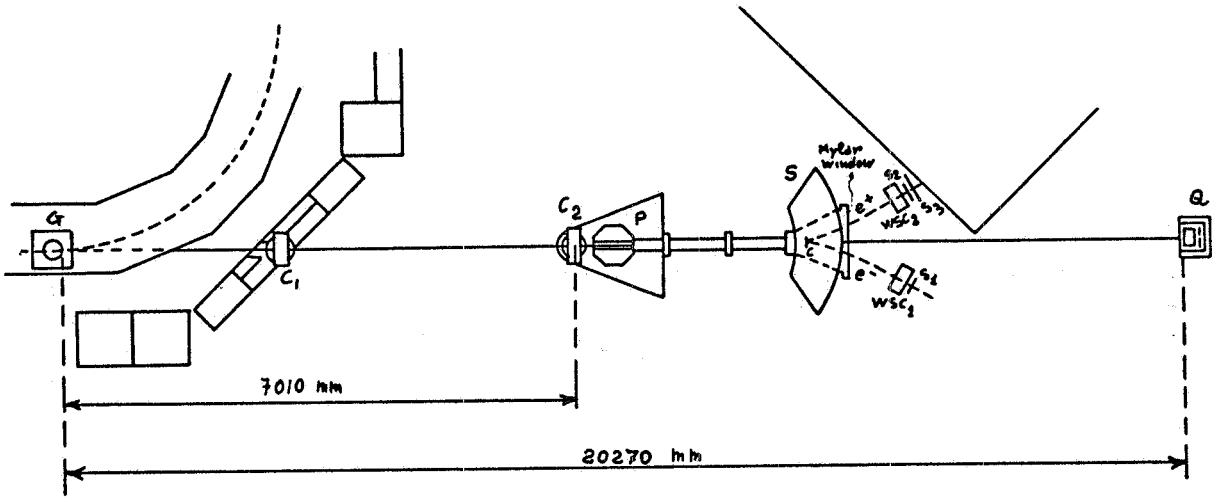

FIG. 1 - Experimental apparatus. G = Goniometer, C_1 = I collimator, ϕ = 5 mm, C_2 = II collimator, ϕ = 3 mm, PS = Pair Spectrometer, S_1, S_2, S_3 = = Plastic scintillation counters, WSC_1, WSC_2 = Wide gap spark-chambers, P = Clearing field, Q = Quantameter.

As shown in Fig. 1, the beam is collimated twice by the two round collimators C_1 and C_2. C_1 reduces the size of the beam lighting C_2 and decreases background source. C_2 gives the effective collimation, that is

$$\theta_{coll} = \frac{1,5 \text{ mm}}{7010 \text{ mm}} \cong 2,1 \cdot 10^{-4} \text{ rad}$$

where θ_{coll} is the half collimation angle. In the aluminium converter C the γ-beam produces electron positron pairs. The converter C is only 10μ thick, in order to reduce the multiple scattering suffered by the pro duced pairs. The detecting apparatus, is also shown in Fig. 1.

The master coincidence between the scintillation counters S_1, S_2, S_3, defining the energy of the symmetric pair (v. Fig. 2) triggers the Marx generator that applies a high voltage pulse to the wide gap spark-chambers. The two wide gap spark-chambers, used in the delineating mode of operation, detect the track left by the electrons trig-

gering the coincidence.

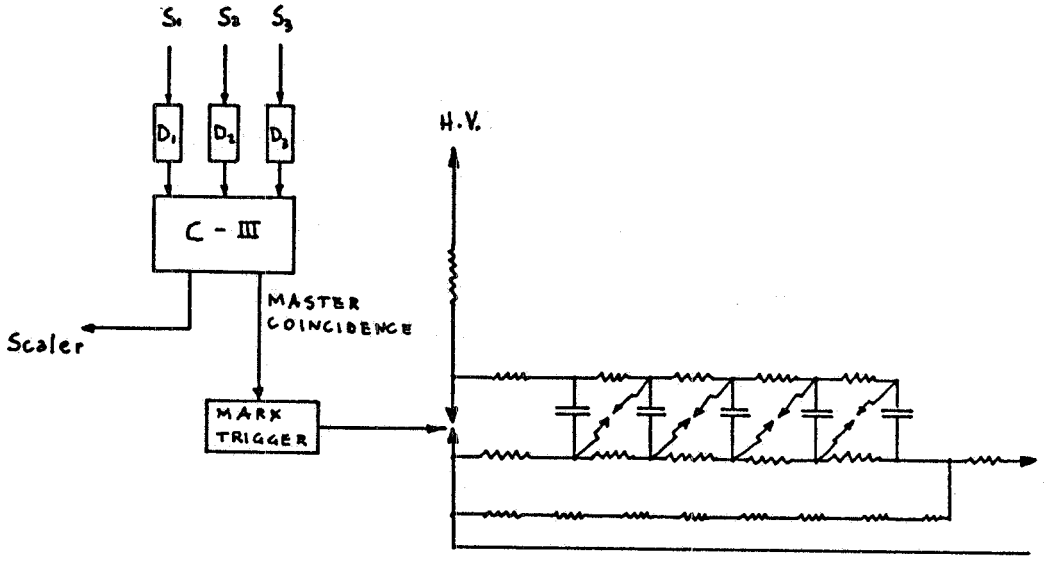

FIG. 2 - Electronic scheme to fire the wide gap spark-chambers. D_1, D_2, D_3 = Discriminators, C_1 III = threshold coincidence. The Marx generator output goes to the wide gap spark-chamber (WSC).

The wide gap spark-chambers WSC_1, WSC_2 ($20 \times 20 \times 10$ cm^3) had thin aluminum foils (0.5 mm) as electrodes, and were continuously fluxed with pure He gas, contained in a rectangular mylar box placed between the electrodes.

Linear fiducial marks define a rectangular frame of reference and the position of the track along the y-axis is measured as shown in Fig. 3.

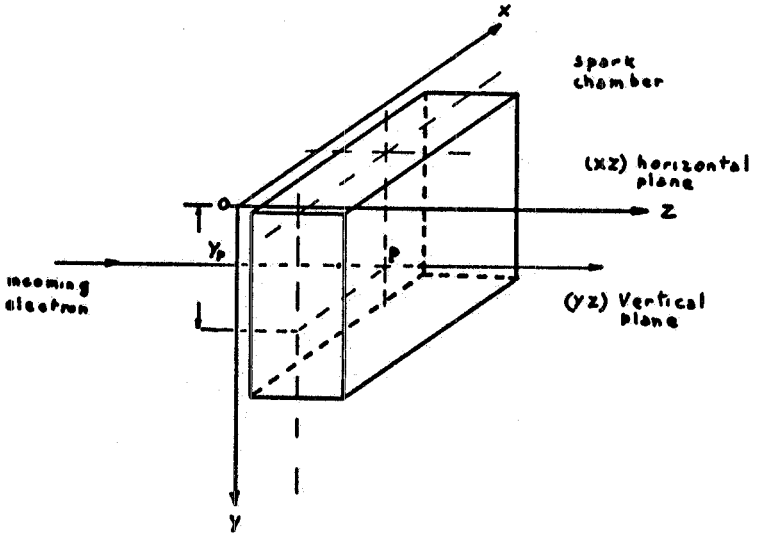

FIG. 3 - Schematic view of the reference frame used to locate the track light by the electron in the WSC.

By using mirrors two rectangular views of the chambers were recorded on Ferrania P30 film using a camera with f/16 lens opening. The x distribution of electrons was used to check resolution energy $\Delta E/E$ of the pair spectrometer.

The chambers were pulsed with a 9 KV/cm electric field, applied between the electrodes by a double five stages Marx generator, with air spark-gaps. The total delay between the ma

ster coincidence $S_1 S_2 S_3$ and the H. V. pulse was about 400 ns.

EXPERIMENTAL RESULTS. -

The γ beam polarization is defined by the quantity

$$P = \frac{I_\perp - I_\parallel}{I_\perp + I_\parallel}$$

were $I_\perp$ and $I_\parallel$ are the number of photons with electric vector $\vec{\mathcal{E}}$ perpendicular or normal to the plane $(\vec{a}_1, \vec{p}_e)$ respectively, where $\vec{a}_1$ is the crystal axis (in our case [110] axis), and $\vec{p}_e$ is the incoming electron momentum.

At fixed angle θ between $\vec{a}_1$ and $\vec{p}_e$, by rotating this plane around $\vec{p}_e$, it is possible to have any polarization orientation with respect to a fixed reference frame.

We have chosen the angle θ in such a way as to have coherent bremsstrahlung and consequently polarization in the energy region around 150 MeV of the γ beam energy spectrum.

In order to select the proper photon energy, the symmetric pair produced by 150 MeV energy photons are magnetically deflected in the pair spectrometer. Due to the magnetic deflection, which measures electron pair energy and consequently photon energy, information on the electron emission angle in the plane normal to the magnetic field $\vec{B}$ is completely lost. What we measure is thus a projected angular distribution in the plane defined by $\vec{B}$ and the photon momentum $\vec{K}$ this plane is coincident with the vertical plane. The same horizontal x coordinate at the wide gap spark-chamber can be obtained by electrons of slightly different production angle with respect to the photon direction and simultaneously slightly different energy.

This situation is roughly sketched in Fig. 4. The horizontal coordinate is mainly a function of electron energy, and of emission angle too.

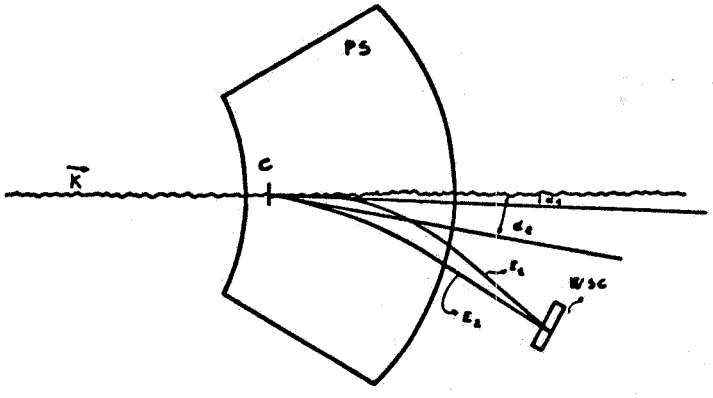

FIG. 4 - Rough skecth to illustrate how two electrons produced at different angles (α_1, α_2) respect to the photon direction K, and with slightly different energies E_1, E_2 can have the same horizontal coordinate at the WSC.

We accept small energy average $\Delta E/E$, where E is the electron energy; this is anyway enough to integrate the projected angular distribution in the horizontal plane.

Fig. 5 shows the theoretical energy spectrum of the bremsstrahlung intensity (i.e., photon energy times number of photon per unit energy interval), from the diamond after the proper orientation has been chosen[2]. The experimental intensity values are measured by the pair spectrometer, as in previous experiments[3], while the theoretical spectrum is corrected for the various experimental effects.

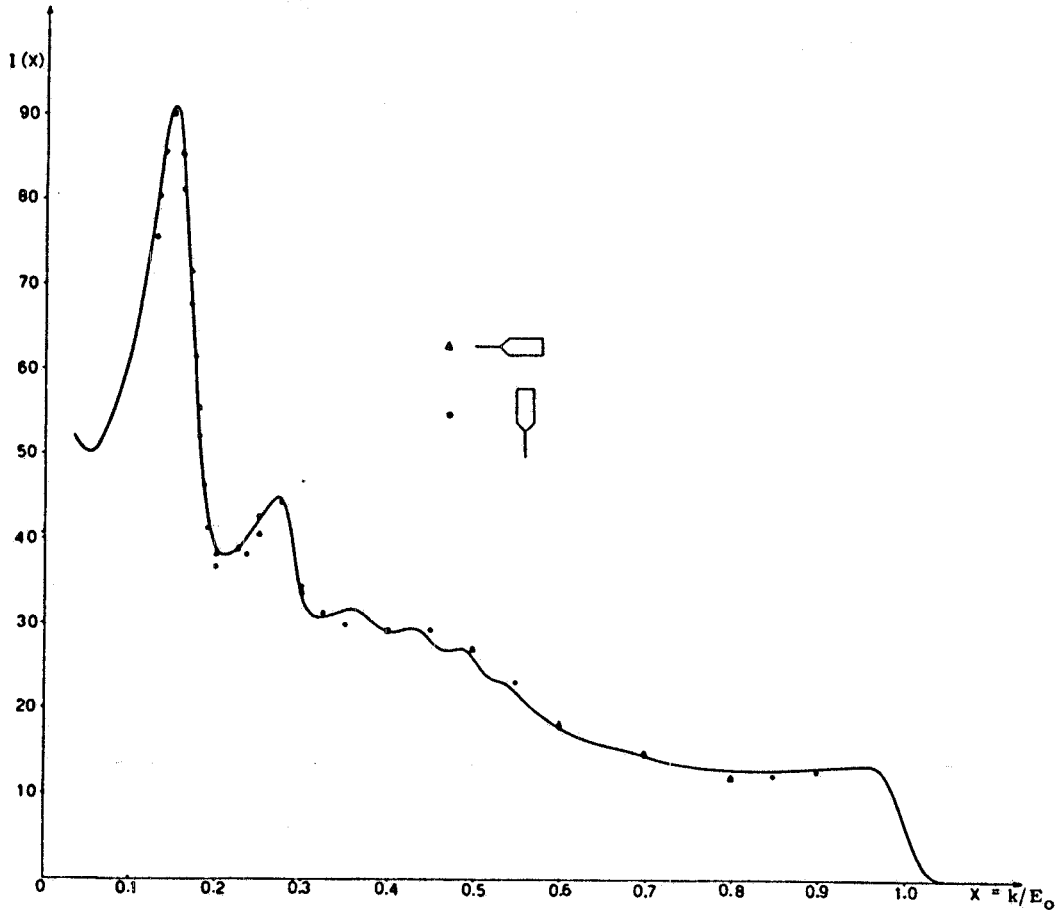

FIG. 5 - Normalized bremsstrahlung intensity of $E_o = 1$ GeV electrons in the two diamonds crystals used alternatively to have vertical and horizontal polarization during the experiment. The two labels refer to each one of the crystal that the are rotated around vertical or horizontal axis. Solid curve is calculated from reference (2). X is the fractional energy K/E_o.

The two spectra are obtained from two diamonds used alternatively to change orientation of polarization vector $\vec{\varepsilon}$, with respect to the vertical plane. The vertical plane is a priviliged plane because it contains the magnetic field as previously mentioned.

The photon energy resolution $\Delta K/K = \Delta E/E$ (K = photon energy, E = electron energy) of our apparatus is determined by the finite dimensions of the plastic scintillation used to detect the electrons.

It would be possible to require a better resolution $\Delta K/K$ by reading the horizontal coordinate x, which is related to E; however this is not necessary in our case because the polarization value P changes smoothly in the range of the values of K, as defined by the plastic counter energy resolution ΔK, (see Fig. 6).

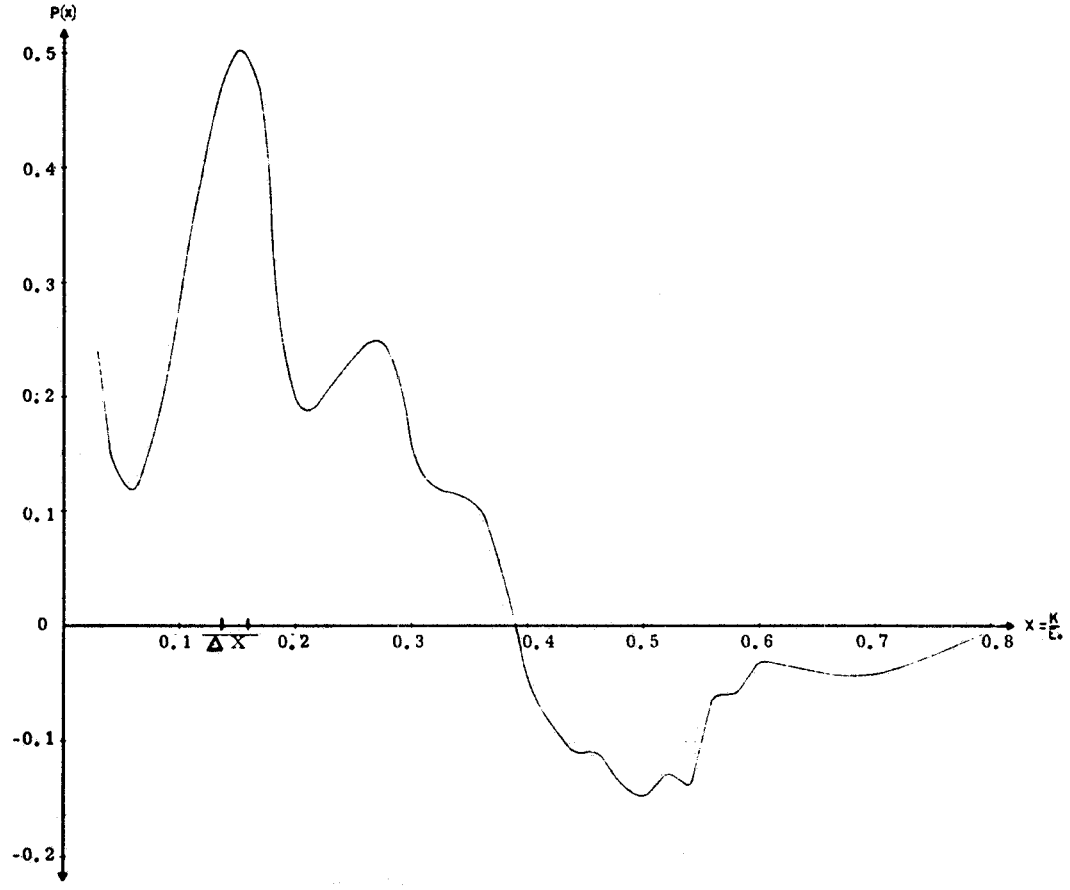

FIG. 6 - Polarization behaviour as a function of the fractional energy X, calculated with diamond in the same situation as for Fig. 5.

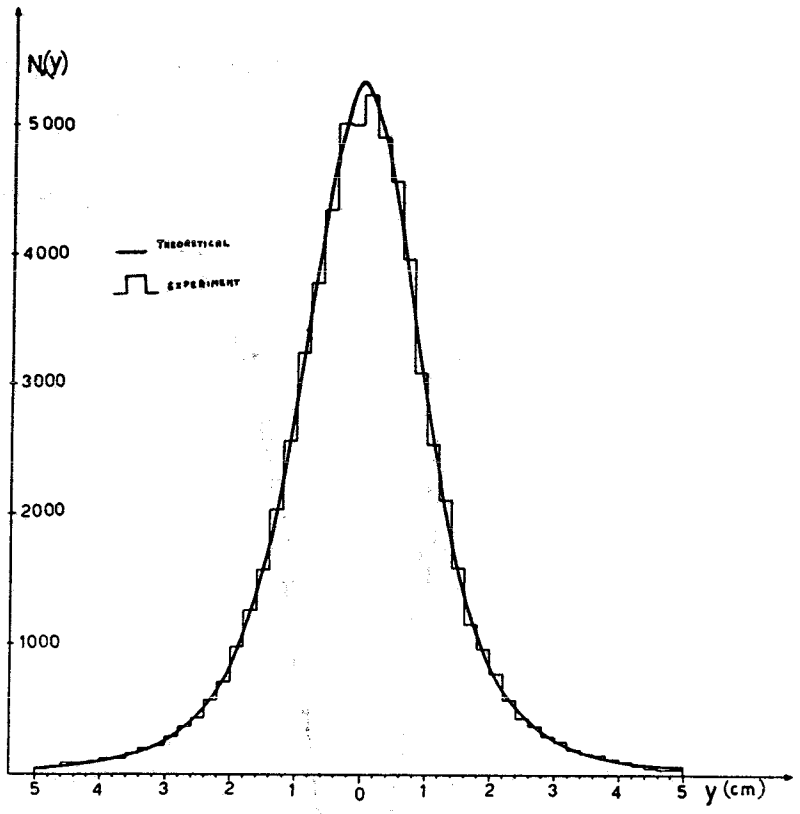

FIG. 7a - Theoretical projected angular distribution

$$f_{\parallel} = \sigma(1 - P\,\frac{\sigma_{\parallel} - \sigma_{\perp}}{\sigma_{\parallel} + \sigma_{\perp}}) \quad \text{at} \quad P = 52\%$$

after scattering is taken in account and correspondent experimental distribution $N_{\parallel}$.

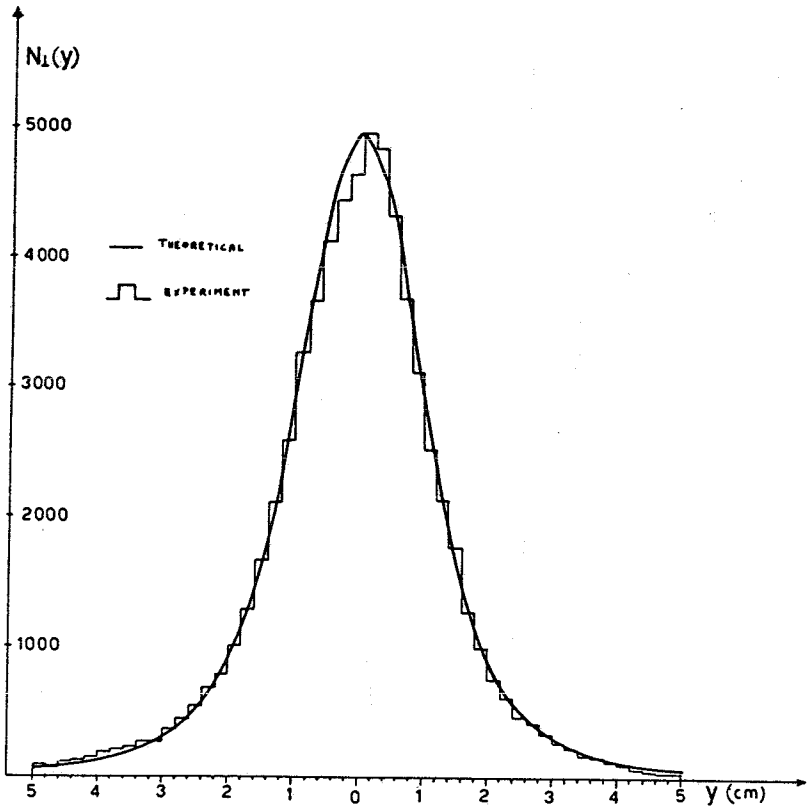

FIG. 7b - Theoretical projected angular distribution

$$f_{\perp} = \sigma(1 - P\,\frac{\sigma_{\parallel} - \sigma_{\perp}}{\sigma_{\parallel} + \sigma_{\perp}}) \quad \text{at} \quad P = 52\%$$

after scattering is taken in account and correspondent experimental distribution $N_{\perp}$.

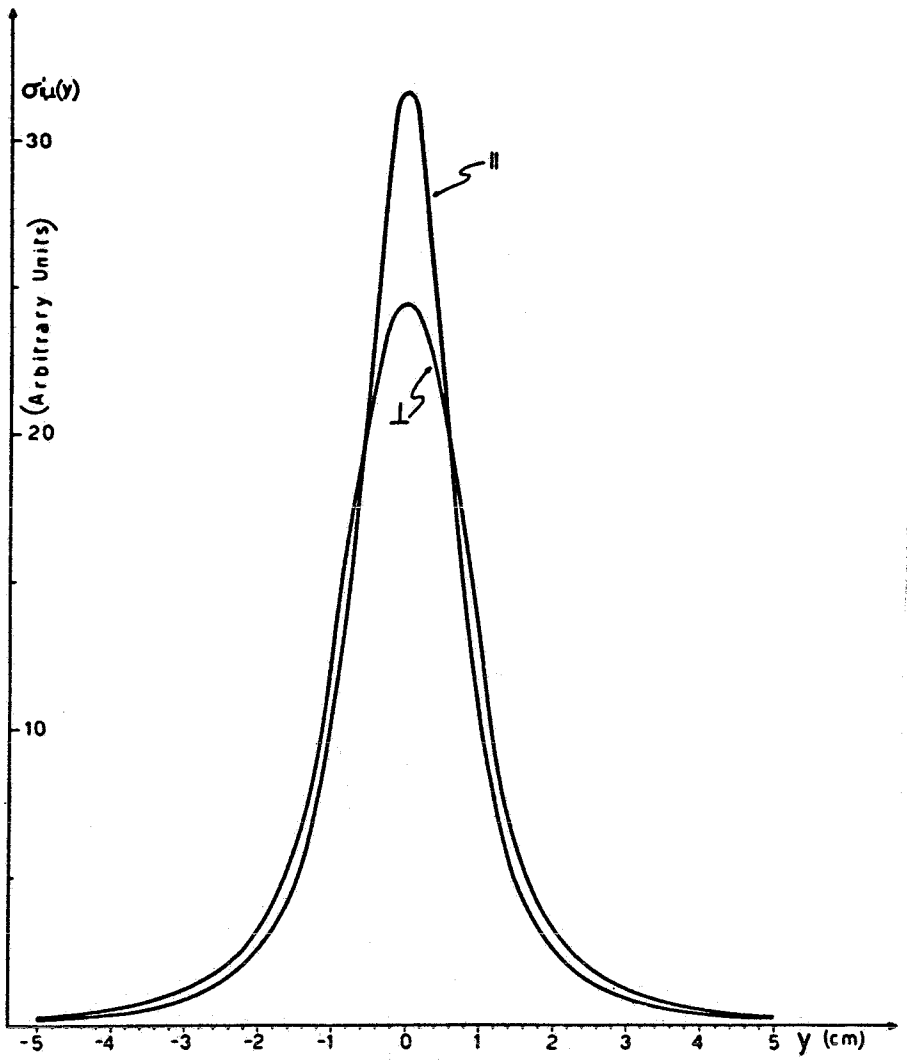

FIG. 8a - $\sigma'_{II,\perp}$ (y) are the theoretical distributions as a function of the vertical coordinate y.

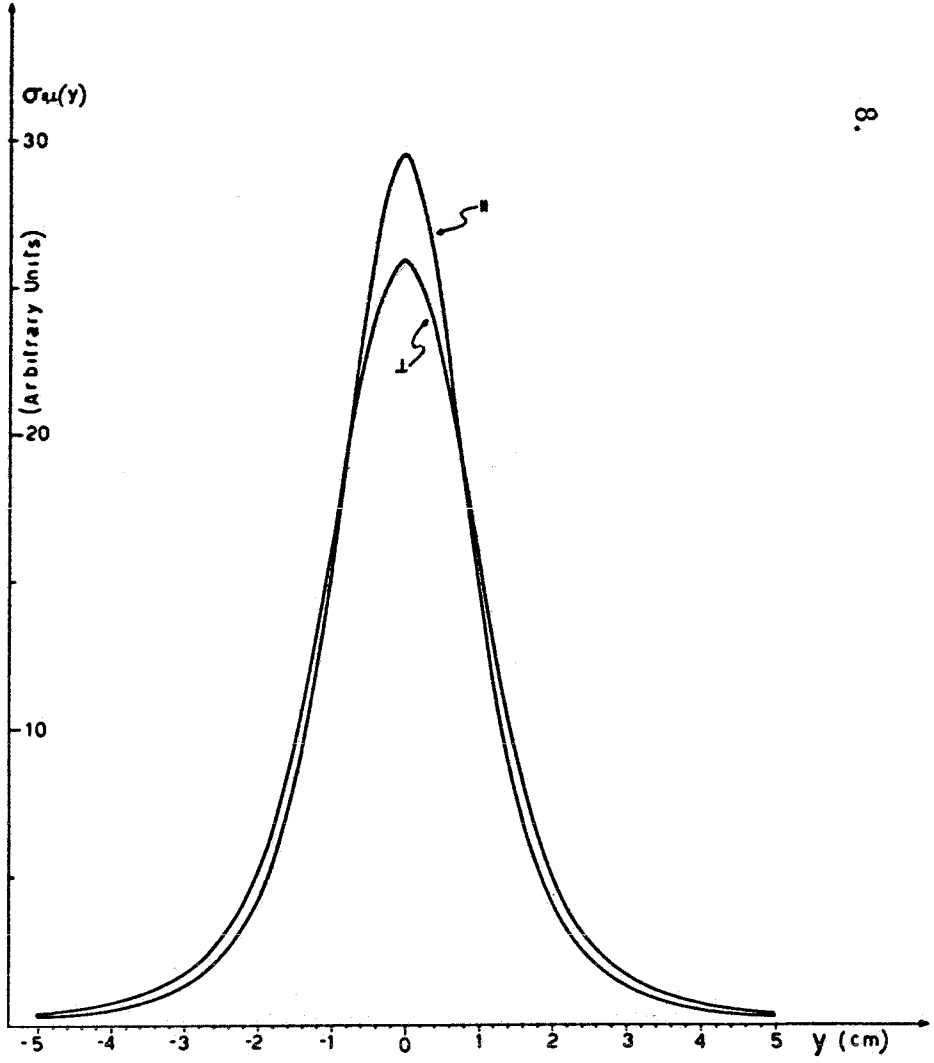

FIG. 8b - $\sigma_{II,\perp}$ (y) are the modification of the distribution shown in Fig. 8a after scattering correction is taken in account.

In Fig. 7(a, b) the distribution of $N_{\parallel}$ (y) and $N_{\perp}$ (y) are plotted.

$N_{\parallel(\perp)}(y)$ are the numbers of events in which one of the electrons of the pair crosses the spark chamber with the coordinate within y, and y+ Δy, and with the polarization plane coincident with the horizontal (vertical) plane. Due to the small aperture of the pair the vertical y coordinate is simply related to the projected angle and to the distance d between the C converter and the scintillation counters (d $\sim$ 2 m). On the other hand, for the same incoming photon flux we have the following equation:

$$\int_0^{\infty} N_{\parallel} \ (y)\, dy = \int_0^{\infty} N_{\perp} \ (y)\, dy \ ,$$

because the total number of events depends only on the total number of incoming photons.

The two distributions $N_{\parallel,\perp}(y)$ are normalized to the same area, i. e. to the same number of incoming photons.

The photon polarization is related to $N_{\parallel}(y=0)\cdot\Delta y$ and $N_{\perp}(y=0)\cdot\Delta y$ through the equation:

$$(1) \qquad P = \frac{1}{A}\,\frac{N_{\parallel} - N_{\perp}}{N_{\parallel} + N_{\perp}} = \frac{1}{A}\,\frac{R_c - 1}{R_c + 1}$$

where

$$A = \frac{\sigma_{\parallel} - \sigma_{\perp}}{\sigma_{\parallel} + \sigma_{\perp}} = \frac{R_\sigma - 1}{R_\sigma + 1}, \quad R_\sigma = \frac{\sigma_{\parallel}}{\sigma_{\perp}} \ , \quad R_c = \frac{N_{\parallel}}{N_{\perp}}$$

and where $\sigma_{\parallel,\perp}$ are the cross sections for the production of a pair integrated over one of the branches and where the production plane of the other branch is parallel or normal to the polarization plane.

The theoretical distribution of the events as function of y and for the two photon polarization states, (parallel or normal to the horizontal plane) has been calculated[4, 5].

Fig. 8a) shows $\sigma'_{\parallel}(y)$, $\sigma'_{\perp}(y)$, the theoretical cross sections, while Fig. 8b shows $\sigma_{\parallel}(y)$, $\sigma_{\perp}(y)$ which have been used in equation (1) and are obtained from $\sigma'_{\parallel,\perp}(y)$, by allowing for multiple scattering in the converter, in the mylar window and in the air gap between mylar window and wide spark-chamber.

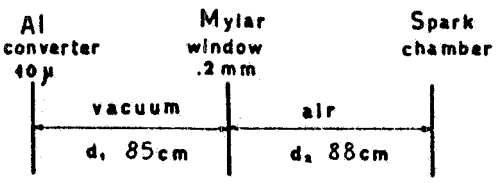

FIG. 9 - Sketch of the scatteres met by the electron before to be detected in the WSC.

The smoothing effect of multiple scattering experienced by the electrons in the scatterers placed before the wide gap spark-chamber (see Fig. 9), was evaluated following Molière's theory of multiple scattering by using a simple program for the IBM 7040 computer.

In Fig. 10 we plot the quantities:

$$f_{\parallel,\perp}(P) = \sigma\left(1 \pm \frac{\sigma_{\parallel} - \sigma_{\perp}}{\sigma_{\parallel} + \sigma_{\perp}} P\right)$$

The two sets of curves are referred to $P_1 = 40\%$ (dashed curves) and $P_2 = 60\%$ (dotted curve).

The experimental results $N_{\parallel,\perp}(\Delta y)$, where $N_{\parallel,\perp}$ are previously defined and Δy is the vertical coordinate bin ($\Delta y = 2$ mm) are shown in Fig. 7. In the same figure are plotted $f_{\parallel,\perp}(P)$, where $P = 52\%$ is the polarization value which gives the best fit to the experimental points.

Theoretical and experimental value are normalized to the same area. The experimental quantity $N = (N_{\parallel} + N_{\perp})/2$ is also compared to the theoretical quantity $f = (f_{\parallel} + f_{\perp})/2$. Both N and f are polarization independent. Fig. 11 shows the agreement between theoretical prevision and experimental results. This agreement is an internal check that insures that scattering effects are properly taken in to account.

The correct scattering evaluation is rather important for polarization measurement because, as shown in Fig. 8b), the difference between the $\sigma_{\parallel}$ and $\sigma_{\perp}$ are sensitive to the amount of scattering suffered by the electrons.

In the first column of the Table I we give the experimental quantity $R_c(\Delta y) = N_{\parallel}(\Delta y)/N_{\perp}(\Delta y)$ versus different values of Δy; in the second, third, and fourth columns the theoretical ratio $R_t = f_{\parallel}(\Delta y, P)/f_{\perp}(\Delta y, P)$ are represented versus Δy and for the following P values:

$$P_1 = 52\% \qquad P_2 = 40\% \qquad P_3 = 60\%$$

TABLE I

Δy (mm)	R_c	$R_t(P_1)$	$R_t(P_2)$	$R_t(P_3)$
2	$1,064 \pm 0,016$	1,073	1,055	1,083
4	$1,062 \pm 0,011$	1,066	1,050	1,076
6	$1,059 \pm 0,009$	1,057	1,043	1,066

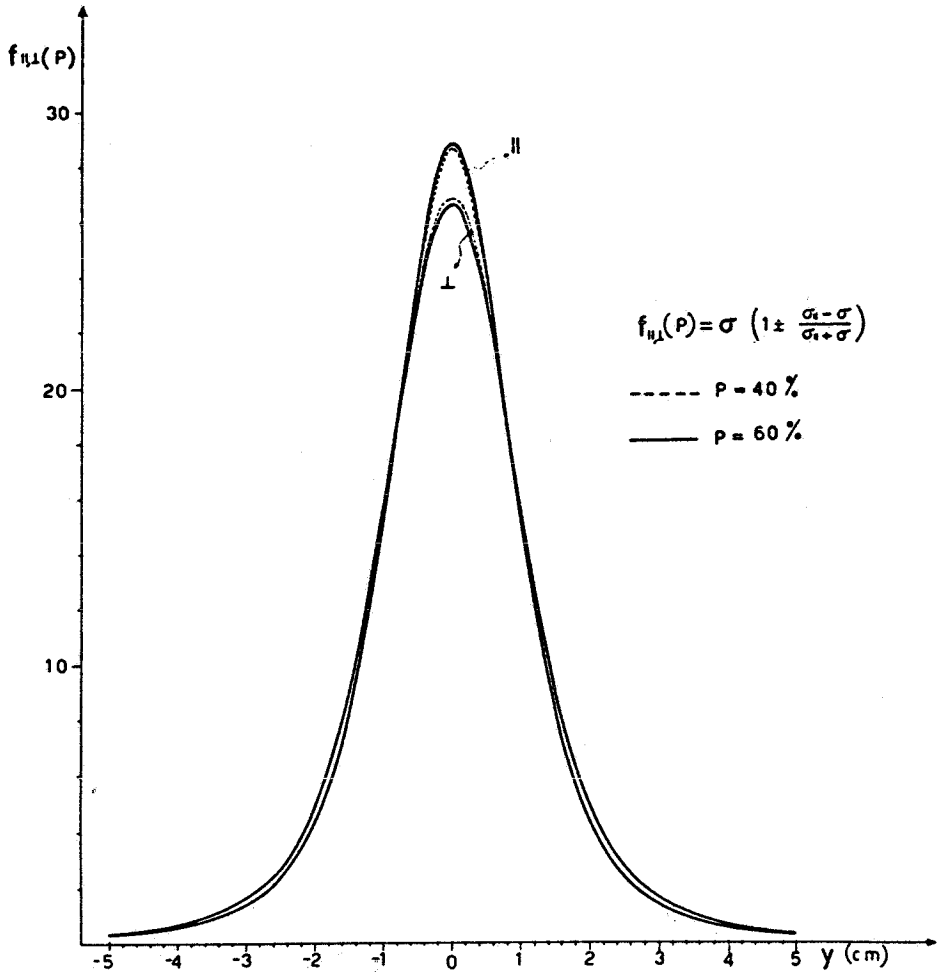

FIG. 10 - Theoretical angular projected distributions $f_{\parallel,\perp}(P, y)$ when scattering is taken in account for the following P values:
a) continuous line P = 60%
b) dotted line P = 40%.

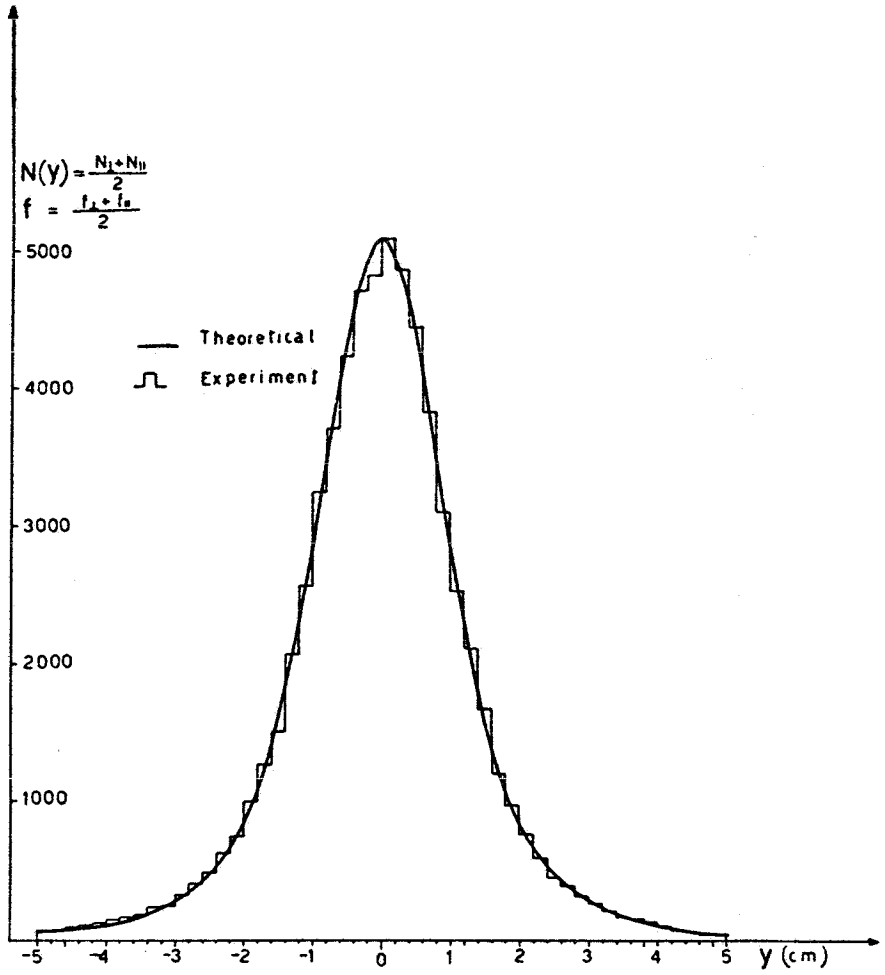

FIG. 11 - Behaviour of the polarization independent quantities

$$N(y) = \frac{N_\parallel + N_\perp}{2} \quad \text{and} \quad f = \frac{f_\parallel + f_\perp}{2}$$

versus the y coordinate. The agreement between the experimental quantity N and the theoretical one f insures that scattering effects are properly evaluated.

The errors on the values of the first column are only statistical. The, values of R_c, $R_t(P_1)$, $R_t(P_2)$, $R_t(P_3)$ versus Δy are shown in Fig. 12.

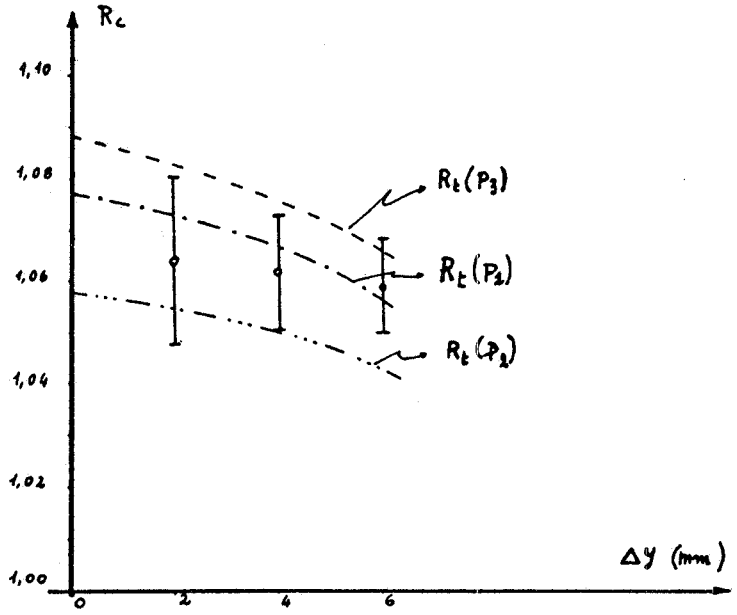

FIG. 12 - Theoretical ratio

$$R_t(P) = \frac{f_{\parallel}}{f_{\perp}}$$

as a function of Δy coordinate range around $y = 0$ and for the three values of P correspondlng to $P_1 = 52\%$ $P_2 = 40\%$ $P_3 = 60\%$ R_c experimental ratio $N_{\parallel}/N_{\perp}$ versus Δy.

The beam polarization which we derive from our measurements by using equation (1) with $\Delta y = .4$ cm, is

$$P = (52 \pm 9)\%$$

This value is in good agreement with the theoretical value $P = 50\%$ (see Fig. 6).

CONCLUSIONS. -

A polarization measurement of 150 MeV energy photons using pair production was previously done by counter technique[6].

We believe that the main differences between the two experiments consists in the following:

first, by measuring all the projected angular distributions, with a visualizing technique, we obtain a polarization independent check, which insures that the scattering effects are properly taken into account (Compare the experiment distribution $(N_{\parallel} + N_{\perp})/2$ and the theoretical $(f_{\parallel} + f_{\perp})/2$).

Second: the new data are independent from possible electronic inefficiency as the same electronic master is used to detect the events which are polarization dependent ($N_{\parallel}$ $(y = 0)$, $N_{\perp}$ $(y = 0)$), as well as the norma-

lization factors $\int N_{\parallel}(y)\,dy$, $\int N_{\perp}(y)\,dy$, which are polarization independent.

ACKNOWLEDGMENTS. -

The comments, suggestions and assistence of Prof. Diambrini, Prof. Bologna and Prof. Murtas are greatfully acknowledged.

We are greatful also to Ing. F. Pandarese who helped us in a preliminary automatic scanning of our events.

REFERENCES. -

(1) - L. C. Maximon and H. Olsen, Phys. Rev. 126, 310 (1962).
(2) - The best working point of the crystal has been chosen following the prescription of G. Bologna, Nuovo Cimento 40A, 756 (1967), by taking $\alpha = 13.26^{o}$, $\beta = 0$. Computation of bremsstrahlung spectrum and polarization was performed by the same author.
(3) - G. Barbiellini, G. Bologna, G. Diambrini and G. P. Murtas, Phys. Rev. Letters 8, 454 (1962); 9, 46 (1962).
(4) - B. Antonini, Thesis (unpublished).
(5) - M. Bartolucci and F. Grianti, Internal Note INFN-66/2 AEB 10 (1966).
(6) - G. Barbiellini, G. Bologna, G. Diambrini and G. P. Murtas, Phys. Rev. Letters 9, 519 (C) (1962).